J Solid State Electrochem (2006) 10: 61–68
DOI 10.1007/s10008-005-0656-8

ORIGINAL PAPER

M. Šupicová · R. Rozik · L. Trnková
R. Oriňáková · M. Gálová

Influence of boric acid on the electrochemical deposition of Ni

Received: 28 September 2004 / Revised: 25 January 2005 / Accepted: 28 January 2005 / Published online: 20 May 2005

Abstract The electrolytic deposition of Ni onto a paraffin-impregnated graphite electrode from supporting chloride electrolyte (0.5 mol dm^{-3} NaCl) adjusted to the required pH using dilute HCl is investigated. The effect of electrolyte composition on the Ni electrodeposition is studied using linear sweep voltammetry in the cathodic region. An elimination voltammetry procedure was applied to evaluate the polarization curves. The aim of this work was to deduce the mechanism of Ni reduction in the chloride bath as well as the influence of boric acid on this. Positively-charged $NiCl^+$ ions were found to be the electroactive particles in the Ni reduction mechanism. The strong competition between the $NiCl^+$, Cl^- and H^+ ions for active sites at the electrode is discussed. Kinetically-controlled adsorption/desorption processes of various species were also confirmed using elimination voltammetry with a linear scan. The evolution of gaseous hydrogen, catalyzed by the freshly-deposited Ni, accompanies the electrodeposition process. The presence of boric acid at a sufficiently high concentration inhibits the deposition of Ni and, at the same time, improves the morphology and brightness, as well as the adhesion of the deposited Ni.

Elimination voltammetry with a linear scan is an efficient way to evaluate current–potential curves that reflect the electrodeposition of one-component Ni coatings. By eliminating selected currents, additional interesting and useful information can be obtained from voltammetric data.

Keywords Ni electrodeposition · Chloride supporting electrolyte · Graphite electrode · Boric acid · Elimination voltammetry

Presented at the conference Solid State Chemistry 2004, September 13–17, Prague, Czech Republic

M. Šupicová (✉) · R. Oriňáková · M. Gálová
Institute of Chemistry, Faculty of Science,
P. J. Šafárik University, Moyzesova 11,
041 54 Košice, Slovak Republic
E-mail: magdas@pobox.sk
Tel.: +421-55-6222605
Fax: +421-55-6222124

R. Rozik · L. Trnková
Department of Physical and Theoretical Chemistry,
Faculty of Science, Masaryk University,
Kotlářská 2, 611 37 Brno, Czech Republic

Introduction

Ni electroplating is a commercially important and versatile surface finishing process. Its commercial importance may by gauged from the amount of Ni in the form of metal and salts consumed annually for electroplating, now roughly 100,000 metric tones worldwide [1]. Ni and its alloys are usually deposited on row surfaces to improve corrosion and wear resistance or to modify magnetic and other properties.

The Ni reduction mechanism used in Watts baths has been the subject of numerous and extensive studies [2, 3]. Many of them have focused on explaining the mechanism of nickel electrodeposition onto various substrates (Ni, Cu, Pt) [4, 5]. Most authors assume a mechanism that involves two consecutive one-electron charge transfer steps and the participation of an anion in the formation of an adsorbed complex. This mechanism can be represented in a general scheme as follows:

$$\begin{aligned} &\text{a) } Ni^{2+} + X^- \leftrightarrow NiX^+ \\ &\text{b) } NiX^+ + e^- \leftrightarrow NiX_{ads} \\ &\text{c) } NiX_{ads} + e^- \leftrightarrow Ni + X^- \end{aligned} \quad (1)$$

The anion X^- was variously assumed to be either OH^- or Cl^-.

The surface adsorptions of metal hydroxyl ions ($NiOH^+$) have been observed and investigated by many researchers [6, 7, 8]. Recent studies have concentrated on investigating any interference of Ni and Fe during Ni-Fe plating in the presence of boric acid, but the influence of the boric acid itself was often overlooked. The effect of

boric acid on the electrodeposition of Fe, Ni and Fe-Ni onto a copper rotating disc electrode was studied by Yin and Lin [9]. Their experimental results support the concept that the boric acid prevents electrode surface passivation during the Ni reduction. Furthermore, the boric acid acts as a surface agent as well as a selective membrane, blocking the reduction of nickel and the evolution of hydrogen but permitting the reduction of iron at a retarded rate.

In our previous work, we studied the influence of the pH at the electrolytes during Ni electrodeposition, using various concentrations of $NiSO_4$, H_3BO_3 and NaCl [10]. The conventional plating Watts electrolyte used in industrial processes consists of $NiSO_4$, H_3BO_3 and NaCl adjusted to pH 2 via H_2SO_4. To investigate the Ni electrodeposition process, as well as the roles of the individual components, we chose linear sweep voltammetry (LSV), cyclic voltammetry (CV) and elimination voltammetry with linear scan (EVLS) techniques. The present contribution is focused on studying the mechanism of the deposition of Ni from a chloride supporting electrolyte onto an inert electrode with large surface area (a paraffin-impregnated graphite electrode, PIGE). There are strong indications that this mechanism depends largely on the type of electrolyte used, as confirmed by the experimental observations mentioned in the ''Results and Discussion'' section.

The electrodeposition of the metal is accompanied by simultaneous evolution of H_2, resulting in an increase in the pH in the vicinity of the electrode surface. The freshly deposited nickel layer acts as a catalyst for the evolution of hydrogen, since it causes a drop in the overvoltage for this process. Therefore, the effect of pH upon the polarization behavior was also investigated. Finally, we also investigated the effect of H_3BO_3 concentration on the simultaneous deposition of Ni and H_2 onto PIGE using EVLS.

EVLS belongs to a family of elimination methods that can be traced back to elimination polarography (EP). Both methods are based on the elimination of unwanted current components from total measured current [11]. The EVLS method has proved to be useful in two ways: firstly, by improving the performance of analytical methods, and secondly, by facilitating investigations of electrode processes. Several works have concentrated on deriving elimination functions and procedures [12, 13, 14].

EVLS is a method of mathematical processing a voltammetric signal. The general idea is based on the elimination of particular currents using a linear combination of total currents measured at different scan rates. One of these is taken as the reference scan rate (v), while the others are chosen as multipliers (v_2) or fractions ($v_{1/2}$) of the reference scan rate:

a) $I_{v_{1/2}}$ = total current measured at $v_{1/2}$

b) I_v = total (reference) current measured at v

c) I_{v_2} = total current measured at v_2 (2)

Each total current recorded at a specific scan rate can be expressed as the sum of the diffusion current (I_d = const. $v^{1/2}$), the kinetic current (I_k = const. v^0), and the charging current (I_c = const. v^1), where const. indicates a constant selected potential:

$$\begin{aligned} &\text{a) } I_{v_{1/2}} = (I_d)_{v_{1/2}} + (I_k)_{v_{1/2}} + (I_c)_{v_{1/2}} \\ &\text{b) } I_v = (I_d)_v + (I_k)_v + (I_c)_v \\ &\text{c) } I_{v_2} = (I_d)_{v_2} + (I_k)_{v_2} + (I_c)_{v_2} \end{aligned} \quad (3)$$

For the simultaneous elimination of $I_c + I_k$ with I_d conserved, we can write Eqs. 4a–f:

$$\begin{aligned} f(I) \leftarrow \boxed{\begin{matrix} a_{1/2}I_{v_{1/2}} \\ aI_v \\ a_2I_{v_2} \end{matrix}} &= a_{1/2}\left(\tfrac{1}{2}\right)^{1/2} I_d + a_{1/2}I_k + a_{1/2}\left(\tfrac{1}{2}\right) I_c \text{ (a)} \\ &= aI_d + aI_k + aI_c \text{ (b)} \\ &= a_2(2)^{1/2} I_d + a_2 I_k + a_2(2) I_c \text{ (c)} \\ &\quad \downarrow \qquad \downarrow \qquad \downarrow \\ &\quad = I_d \qquad = 0 \qquad = 0 \\ I_d = a_{1/2}\left(\frac{1}{2}\right)^{1/2} I_d + aI_d + a_2(2)^{1/2} I_d &\text{ (d)} \\ 0 = a_{1/2}I_k + aI_k + a_2 I_k &\text{ (e)} \\ 0 = a_{1/2}\left(\frac{1}{2}\right) I_c + aI_c + a_2(2) I_c &\text{ (f)} \\ f(I) = a_{1/2}I_{v_{1/2}} + aI + a_2 I_{v_2} &\text{ (g)} \end{aligned} \quad (4)$$

Therefore, the elimination of the selected particular current (in this case $I_c + I_k$) from the linear scan voltammetry results can be achieved using an elimination function. This function (Eq. 4d) is obtained by a linear combination of total currents measured at mentioned different scan rates ($I_{v_{1/2}}$, I and I_{v_2}), Eq. 4g [11, 12].

The elimination coefficients $a_{1/2}$, a, a_2 are calculated using the three equations 4d–f). To evaluate CV from the elimination functions derived so far [11], the following two elimination functions were applied:

E1: Eliminate I_k, retain I_d, and multiply by $1.707I_c$:

$$f(I) = 3.4142I - 3.4142I_{1/2} \quad (5)$$

E4: Eliminate I_k and I_c and retain I_d:

$$f(I) = 17.485I - 11.657I_{1/2} - 5.8284I_2 \quad (6)$$

The E1 and E4 elimination functions were chosen in order to gain insight into the kinetic phenomena that accompany the electrochemical process and thus explain some details of its mechanism. These theoretical elimination functions have been verified experimentally in systems with hanging mercury drop electrodes [13, 14]. However, the application of the elimination procedure to a system with a solid graphite electrode, as described here, has not been reported previously.

Experimental

Cyclic voltammetry measurements were performed using an AUTOLAB Electrochemical Instrument (EcoChe-

mie, The Netherlands) connected to a VA-Stand 663 (Metrohm, Zurich, Switzerland). All CV curves were recorded at room temperature at three scan rates—7.5, 15 and 30 mV/s—in order to be able to apply the EVLS evaluation method. The electrochemical cell comprised the PIGE working electrode, an Ag/AgCl/3 mol dm^{-3} KCl reference electrode, and a Pt wire auxiliary electrode. Before each experiment, the surface of the PIGE was mechanically renewed with emery paper, polished with glossy paper, and rinsed with distilled water. The reference electrode was separated from the cell via a salt bridge containing supporting electrolyte.

Electrolytes with the following compositions were investigated:

0.5 mol dm^{-3} NaCl (supporting electrolyte)
0.5 mol dm^{-3} NaCl + 1×10^{-3} or 5×10^{-3} or 10×10^{-3} mol dm^{-3} $NiCl_2$
0.5 mol dm^{-3} NaCl + 1×10^{-3} mol dm^{-3} $NiCl_2$ + 1×10^{-4} or 1×10^{-3} or 1×10^{-2} mol dm^{-3} H_3BO_3

All electrolytes were adjusted to the required pH using dilute HCl.

An optical microscope (ZBD 222 ZoomMaster, Prior, Cambridge, England) was used to observe the Ni coating at 120× microscopic enlargement.

Results and discussion

Supporting electrolyte NaCl + HCl

Figure 1a shows the CV record of the supporting electrolyte, 0.5 M NaCl, adjusted to pH 2, at the PIGE electrode. In comparison with supporting electrolyte currents recorded in electrolytes containing both sulfate and chloride ions [10], a negative shift in the potential of the cathodic current of about 400 mV is observed in the present chloride supporting electrolyte. It may be assumed that the specific adsorption of Cl^- at the porous PIGE is greater than at metal electrodes applied in most previous studies [4]. The specific adsorption of chloride ions was also observed in [15] on the surface of a steel electrode. The Cl^- ions occupying the surface of PIGE are released at sufficiently negative potentials, allowing the reduction of hydrogen ions to proceed. We can see from Fig. 1a that the current derived from this reaction at the chosen potential is almost independent of scan rate, which indicates the kinetic character of the process. The EVLS results shown in Fig. 1b, the course of both elimination functions (E4 and E1) at the onset of hydrogen evolution (at positive potentials), confirm the kinetic character of the electrode process. The differences between the E4 and E1 elimination functions may be ascribed to the influence of charging current, an adsorption/desorption process being the rate-determining step.

Many studies have been devoted to the mechanism of hydrogen evolution reaction (such as those of Tafel, Volmer, Heyrovský, Parsons, Gerischer, Horiuti, Okamoto, Bockris; see [16]). This mechanism is influenced by many parameters, mainly by the material and the state of electrode surface, the applied potential, and the current density. Our earlier results in sodium sulfate supporting electrolyte enable us to compare hydrogen evolution in both chloride and sulfate solutions [17]. These results demonstrate that the well-known adsorption of chloride ions onto a Pt electrode [5] can also be observed on a PIGE electrode; thus, the adsorption of Cl^- onto the PIGE shifts both the adsorption of hydrogen and its reduction to more negative potentials. Not only the kinetic character of this cathodic process at the onset of hydrogen reduction, but also the adsorption/desorption character at more negative potentials, as proved by elimination functions E1 and E4, can probably be ascribed to this competition between Cl^- and H^+ ions. Hence, at the experimental conditions applied in the present study, relatively strong adsorption of hydrogen onto the surface of the applied electrode may be assumed. The adsorption of hydrogen takes place only at negative potential, where the competition between the chloride ions and hydrogen for adsorption sites at the electrode is

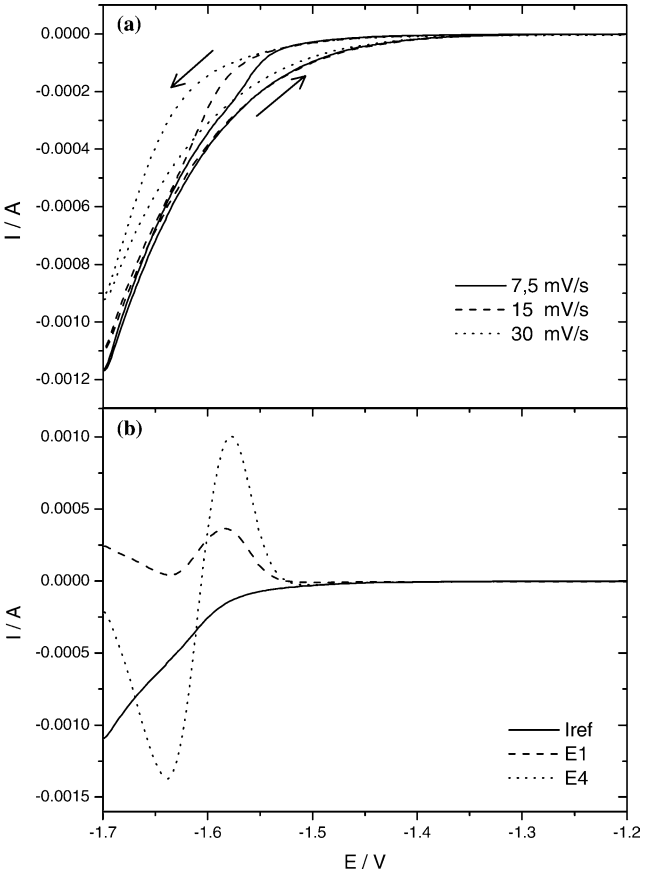

Fig. 1 **a** Cyclic voltammetry record for the supporting electrolyte (0.5 mol dm^{-3} NaCl), adjusted to pH 2 using HCl, at the graphite electrode (PIGE). The reference electrode was Ag/AgCl/3 mol dm^{-3} KCl); scan rates were 7.5, 15, 30 mV/s; potential step was 2 mV. **b** Elimination voltammetric treatment for the record shown in **a**; *E1*, elimination function eliminating kinetic current and conserving diffusion current (charging current is distorted); *E4*, elimination function eliminating kinetic and charging currents and conserving diffusion current

won by the latter. Similar behavior to this was also observed by Goméz et al [5] on Pt and Ni electrodes.

The hydrogen evolution reaction may be considered to consist of two steps: hydrogen adsorption onto the electrode M, combined with the first electron transfer (reaction 7a), followed by electrochemical desorption and transfer of the second electron (7b):

$$\text{a) } M(e) + H_3O^+ + e \rightarrow MH_{(ads)} + H_2O$$
$$\text{b) } MH(ads) + H_3O^+ + e \rightarrow M + H_2 + H_2O \qquad (7)$$

Assuming rather strong adsorption of the MH particle, which both the product in reaction 7a and the reactant in reaction 7b, the transfer of the second electron accompanied by the desorption of molecular hydrogen is probably the slow step, mainly at more negative potentials. The elimination procedure presented in Fig. 1b confirms this assumption.

Reduction of Ni^{2+} ions in the chloride electrolyte, pH 2

The electrolytic reduction of Ni^{2+} from the above electrolyte is presented in Fig. 2a. In these curves, the following effects may be observed: the deposition potentials are shifted towards more positive values as the Ni^{2+} concentration increases; the peak height does not increase in proportion to the increase in Ni^{2+} concentration; following the Ni^{2+} reduction peak, the deposition of hydrogen takes place at potentials that more positive than those in the supporting electrolyte alone; the current associated with hydrogen reduction is proportional to the peak height of nickel reduction.

The elimination procedures E4 and E1 presented in Fig. 2b first show kinetic control at the onset of the Ni^{2+} reduction wave, then adsorption/desorption control at more negative potentials, and finally diffusion control at even more negative potentials. It is worth noting that the elimination procedure increases the peak current by a factor of eight, making the evaluation and analysis of current–potential curves much easier and more accurate.

The dependence of the reduction peak height on the scan rate is presented in Fig. 3, and its analysis proves the pseudo-diffusion character of the peak, which gives the slope of the log current–log scan rate line, v, as 0.516, according to the Randless-Ševčík equation.

In order to remove these processes from the sequence and thus also the reaction mechanism, a distribution diagram was constructed representing the participations and concentrations of all of the compounds present in the electrolyte in the respective concentrations. The results presented in Fig. 4 show the presence of all three Ni(II)-containing compounds, Ni^{2+}, $NiCl^+$, and $NiCl_2$, at very similar concentrations. Exact values for the concentrations of these Ni-containing species in the three electrolytes at various $NiCl_2$ concentrations are presented in Table 1.

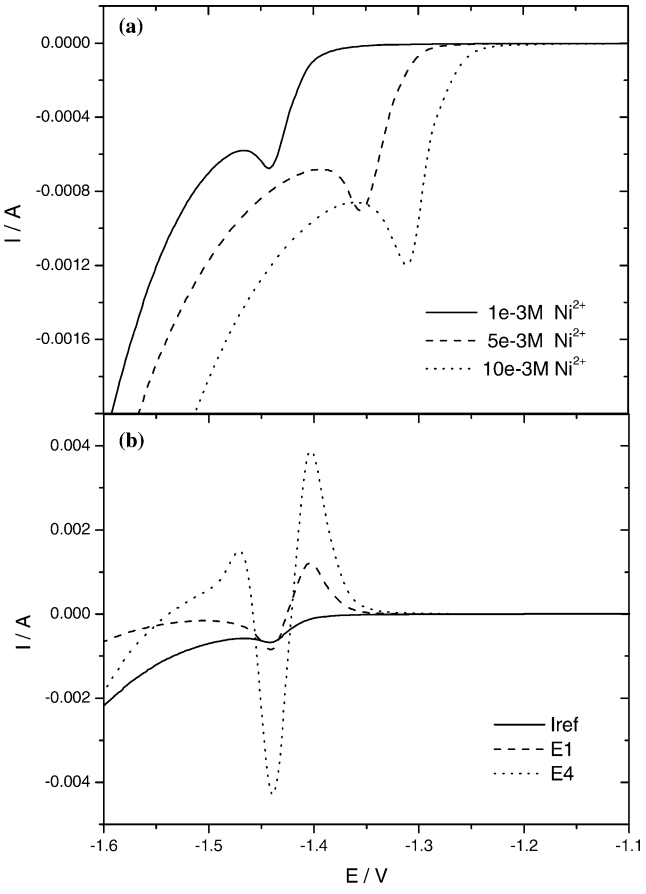

Fig. 2 **a** Cathodic parts of the cyclic voltammograms for Ni reduction at PIGE for various concentrations of $NiCl_2$. Supporting electrolyte was 0.5 mol dm^{-3} NaCl with HCl added to achieve pH 2; scan rate 15 mV/s; other experimental conditions as Fig. 1. **b** Elimination functions E1 and E4 for the voltammogram recorded for **a** with 1×10^{-3} mol dm^{-3} Ni^{2+}; reference scan rate was 15 mV/s

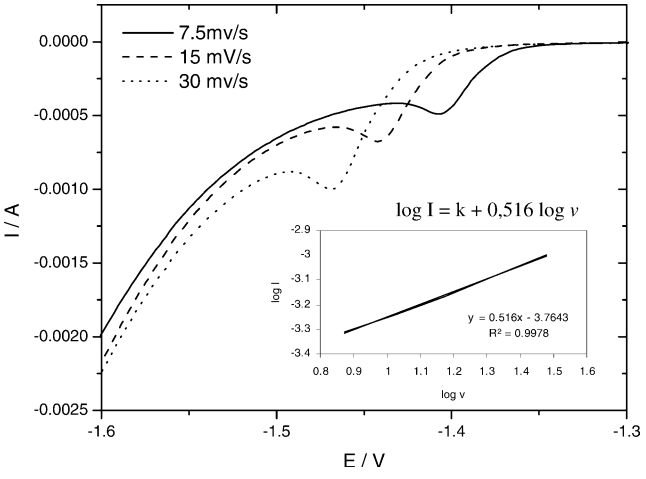

Fig. 3 Change in the voltammetric record of 1×10^{-3} mol dm^{-3} $NiCl_2$ with scan rate; other experimental conditions as in Fig. 1

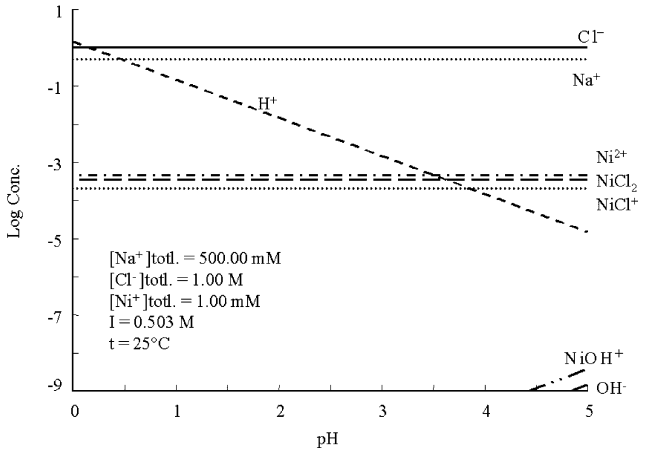

Fig. 4 Distribution diagram for the particles present in an electrolyte consisting of 0.5 mol dm^{-3} NaCl and 1×10^{-3} mol dm^{-3} $NiCl_2$

Following the reasoning of Bockris [18], the particle most likely to be electroactive at the start of Ni electroreduction is the univalent NiX^+ particle, in our case $NiCl^+$. Accordingly, the mechanism of Ni reduction from chloride electrolyte can be expressed as:

$$\begin{aligned} &\text{a)}\quad NiCl^+ \rightarrow NiCl^+_{ads} \\ &\text{b)}\quad NiCl^+_{ads} + e^- \rightarrow NiCl_{ads} \\ &\text{c)}\quad NiCl_{ads} + e^- \rightarrow Ni + Cl^- \end{aligned} \qquad (8)$$

The dependences shown in Fig. 1 imply strong competition between the particles for the active sites on the electrode surface; the positive $NiCl^+$ particles undergo reduction at sufficiently negative potentials only after the chloride ions specifically adsorbed at the electrode have been released. This process, however, is inhibited and shows kinetically-controlled adsorption in the elimination treatment. According to our preliminary results, the kinetic character of the current in the elimination E4 decreases with increasing concentration of the electroactive $NiCl^+$ particles, which is in accordance with the positive shift of the Ni reduction peak with increasing Ni concentration (Fig. 2a).

The deposition of metallic Ni also influences the deposition of H_2 by decreasing the H_2 overvoltage. Consequently, the new Ni layer acts as a catalyst to H_2 evolution. Therefore, the mechanism of H_2 evolution during Ni electrodeposition from chloride medium can be written as follows:

$$\begin{aligned} &\text{a)}\ Ni + H_3O^+ + e^- \leftrightarrow Ni\text{ - }H_{(ads)} + H_2O \\ &\text{b)}\ H_3O^+ + Ni\text{ - }H_{(ads)}e^- \leftrightarrow Ni + H_{2(ads)} + H_2O \\ &\text{c)}\ nH_{2(ads)} \rightarrow (H_2)_n \end{aligned} \qquad (9)$$

The evolution of hydrogen induced by the freshly-deposited Ni layer can be seen in Fig. 2a as an increase of the hydrogen evolution current immediately following the Ni reduction. This increase is proportional to the peak height of Ni, and is shifted to more positive potentials in comparison with the same reaction in supporting electrolyte (Fig. 1a). The mechanisms described by reactions 8a–c and 9a–c are also supported by EVLS results (Fig. 2b). Application of elimination function E4 enables us to detect two proceeding processes: (i) The same courses for the E4 and E1 elimination curves indicate the kinetic current [19], which can be assigned to the kinetically-controlled adsorption of the electroactive particle $NiCl^+$ (8a), made possible only after desorption of Cl^- ions. Earlier experiments have confirmed that the character of the electrode surface and the non-uniform distribution of surface energy at the different active sites influence this process and change the polarization behavior of the E4 elimination curve [20]. (ii) Another elimination result—the peak–counter peak signal of the E4 function—corresponds to the reaction of the electroactive substance adsorbed onto the electrode surface [13, 19]. This surface effect may explain the fact that the Ni reduction current is not proportional to the concentration of Ni particles in the solution. Most likely, the surface concentration of the electroactive particles plays a deciding role.

Table 1 Concentrations of three Ni(II)-containing species (Ni^{2+}, $NiCl^+$,and $NiCl_2$) with increasing $NiCl_2$ concentration, taken from distribution diagrams

$[NiCl_2]$ (mmol dm^{-3})	Concentration of species at pH2, from distribution diagram		
	$\log[Ni^{2+}]$	$\log[NiCl_2]$	$\log[NiCl^+]$
1	−3.36	−3.47	−3.73
5	−2.63	−2.75	−3.03
10	−2.35	−2.74	−2.75

Influence of pH

The influence of pH is demonstrated in Figs. 5a and 5b. The potential of the Ni deposition peak is significantly shifted to more negative potentials as the concentration of H^+ ions increases (in other words, with decreasing pH), and the peak height increases at the same time. The elimination procedure E4 (Fig. 5b) confirms increased kinetic control with increasing H^+ concentration. Both effects, the increased kinetic control and the negative shift of potential, can most likely be attributed to the high concentration of H^+ ions near the electrode, which represent a coulombic barrier to the access of positive $NiCl^+$ particles to the electrode. With increasing Ni concentration, the process requires less energy, and the opposite effect may be encountered: the peak potential shifts in the positive direction (Fig. 2a). The limited peak height proves the surface concentration dependence of the process.

It should be noticed that the reduction of Ni at pH 4 was observed to be different to the reduction that occurred at pH 2 and pH 3. At pH 4, the formation of

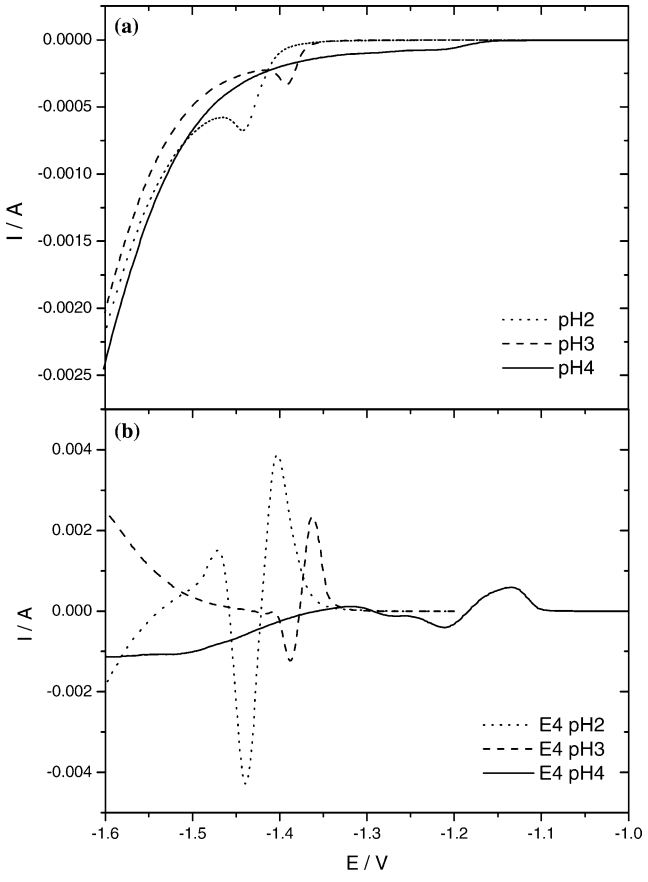

Fig. 5 **a** Voltammetric signal from 1×10^{-3} mol dm^{-3} $NiCl_2$ on PIGE at different pH; supporting electrolyte was 0.5 mol dm^{-3} NaCl with HCl added; scan rate was 15 mV/s; other experimental conditions as Fig. 1. **b** E4 elimination voltammograms (eliminating kinetic and charging currents and conserving diffusion current) for the LSV curves in **a**

solid nickel hydroxide at the electrode surface as a secondary product of Ni reduction cannot be neglected. An inhibitory effect related to the precipitation of nickel hydroxide has been previously detected on vitreous carbon electrodes [21, 22], and is related to pH variations at the electrode interface. The presence of hydroxide was also confirmed by chemical analysis where the deposition product was dissolved in dilute NH_4OH; only the inhibiting salt-containing part of the layer is dissolved, not the metallic part of it [23].

Influence of boric acid

It is well known that boric acid acts as a buffer, in our case stopping the alkalization process in the vicinity of the electrode due to the hydrogen evolution. Moreover, several publications have confirmed that the boric acid acts as a surfactant, which adsorbs on the surface. At the same time, it has also been found that boric acid interferes with metal nucleation processes [24, 25]. The authors attributed the observed changes in surface morphology to a weak boric acid adsorption mechanism.

Our experiments confirmed that a low concentration of H_3BO_3 does not influence the reduction process in the supporting electrolyte. Thus, the adsorption of Cl^- ions is unaffected. With increasing concentrations of H_3BO_3, however, the Ni reduction is shifted to more negative potentials, and, at the same time, the peak height slightly increases, as can be seen in Fig. 6a. A dramatic shift in potential as well as an obvious increase in the peak height may, however, be seen if the H_3BO_3 concentration becomes higher that the concentration of Ni in the solution. Similar interesting results are shown by the E4 elimination procedure in Fig. 6b: the kinetic control of the current observed at the onset of the electrode process initially decreases with low boric acid concentrations, but as the boric concentration rises above the Ni concentration, it shows a dramatic increase as well as a shift in potential. Slow kinetically-controlled adsorption is observed without H_3BO_3 addition. As the H_3BO_3 concentration is increases, it initially acts as a buffering agent, attracting OH^- ions formed near the electrode as a consequence of H_2 evolution; excess H_3BO_3 is most likely adsorbed onto the surface as a neutral molecule strongly inhibiting the reduction of Ni and shifting its

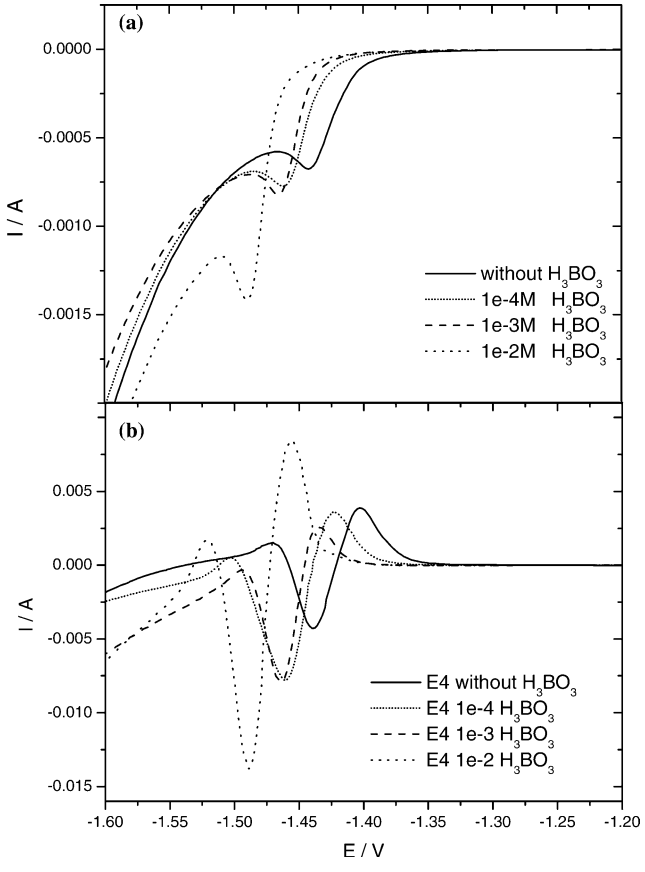

Fig. 6 **a** Effect of various concentrations of H_3BO_3 on the reduction signal from 1×10^{-3} mol dm^{-3} $NiCl_2$ on PIGE. The supporting electrolyte was 0.5 mol dm^{-3} NaCl with HCl added to achieve pH 2; scan rate 15 mV/s; other experimental conditions as in Fig. 1. **b** E4 elimination functions (eliminating kinetic and charging currents and conserving diffusion current) of the records in **a**

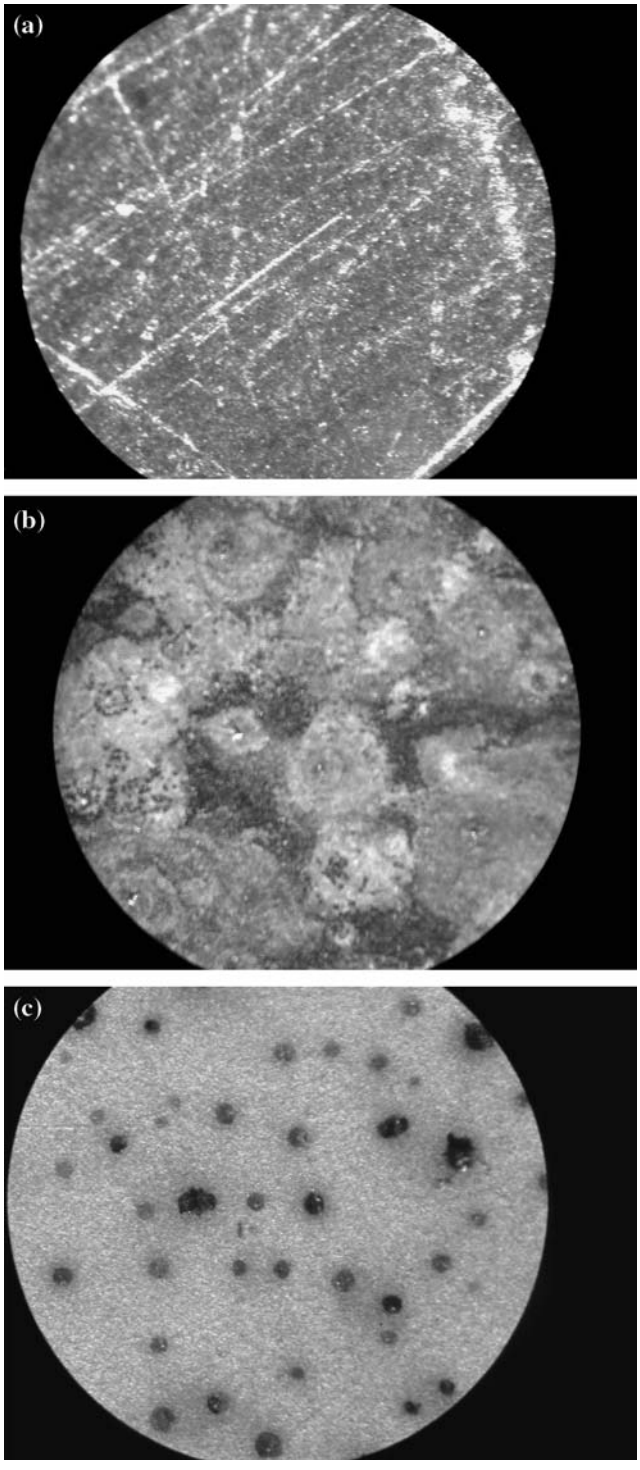

Fig. 7a–c Optical micrographs. **a** Prior to electrolysis, the surface of PIGE was mechanically renewed with emery paper, polished with glossy paper and rinsed with distilled water; the surface is shown here at 120× enlargement. **b** The surface of the PIGE electrode coated with Ni from the 0.5 mol dm^{-3} NaCl + 0.091 mol dm^{-3} $NiCl_2$ electrolyte without H_3BO_3; scan rate 10 mV/s; deposition time 5 min; deposition potential −1140 mV; 120× enlargement shown. **c** The surface of PIGE coated with Ni from the 0.5 mol dm^{-3} NaCl + 0.091 mol dm^{-3} $NiCl_2$ + 0.1 mol dm^{-3} H_3BO_3 electrolyte, pH2; scan rate 10 mV/s; deposition time 5 min; deposition potential −1150 mV; 120× enlargement shown

potential negatively. On the other hand, the adsorption of H_3BO_3 onto the electrode surface seems to inhibit the growth of Ni nuclei, which is associated with higher nucleation rates. A comparison of the optical micrographs in Figs. 7b (without H_3BO_3) and 7c (with H_3BO_3) shows a remarkably refined Ni coating structure in the presence of boric acid. The dark sites in Fig. 7c represent bubbles of hydrogen.

Conclusions

In the process of electrochemical deposition of Ni from a chloride supporting electrolyte on PIGE, the adsorption/desorption processes of various species play a crucial role. Linear and cyclic voltammetry completed by suitably chosen elimination procedures enable us to clarify the mechanism involved to a large extent. Electrochemical experiments were complemented by optical micrographs.

In the supporting electrolyte containing NaCl, the adsorption of chloride ions was detected. Their release from the surface (desorption) at negative potentials enabled deposition of hydrogen from the supporting electrolyte.

The reduction of Ni proceeds from $NiCl^+$ particles and is strongly influenced by the competition between these particles, hydrogen and chloride ions for unoccupied electrode surface sites. This effect is proved by the kinetically-controlled adsorption/desorption process identified using the elimination procedures.

Increasing the H^+ ion concentration produces a similar effect on the Ni reduction process to increasing the H_3BO_3 concentration: it shifts the reduction peak to more negative potentials, and increases the peak height. In addition to this effect, a sufficiently high concentration of H_3BO_3 enhances the Ni nucleation process, which results in an improved deposition.

Acknowledgements This research was supported by Czech-Slovak Cooperation Grant No. 046, the Grant Agency of the Slovak Republic (Grant No. 1/2118/05), and the research project IN-CHEMBIOL (MSM 0021622412) from the Ministry of Education, Youth and Sports of the Czech Republic and MSMT 750/2005.

References

1. Shlesinger M, Paunovic M (2000) Modern electroplating, 4th edn. Wiley, Etobicoke, ON, Canada, pp 139
2. Bozhkov Chr, Tzvetkova Chr, Rashkov St (1990) J Electroanal Chem 296:453
3. Abyaneh MY, Visscher W, Barendrecht E (1983) Electrochim Acta 28:285
4. Saraby-Reintjes A, Fleischmann A (1984) Electrochim Acta 29:557
5. Goméz E, Pollina R, Vallés E (1995) J Electroanal Chem 386:45
6. Hessami S, Tobias CW (1989) J Electrochem Soc 136:3611
7. Beltowska-Lehman E, Riesenkampf A (1980) Surf Technol 11:349
8. Matlosz M (1993) J Electrochem Soc 140:2272

9. Yin KM, Lin BT (1995) Surf Coat Technol 78:205
10. Trnková L, Friml J, Dračka O (2001) Bioelectrochemistry 54:131
11. Dračka O (1996) J Electroanal Chem 402:19
12. Trnková L, Dračka O (1996) J Electroanal Chem 413:123
13. Trnková L, Kizek R, Dračka O (2000) Electroanalysis 12:905
14. Oriňáková R, Trnková L, Gálová M, Šupicová M (2004) Electrochim Acta 49:3587
15. Mirkova L, Maurin G, Monev M, Tsvetkova Chr (2003) J Appl Electrochem 33:93
16. Erdey-Grúz T (1972) Kinetics of electrode processes. Akadémiai Kiadó, Budapest, pp 197
17. Oriňáková R, Šupicová M, Trnková L, Gálová M, Rozik R (2004) Electrochim Acta 49:3587
18. Bocris JOM, Reddy AKN (1970) Modern electrochemistry, vol 2. Plenum, New York, pp 1083
19. Trnková L (2005) J Electroanal Chem (in press) (online: JMF04156F)
20. Rozik R, Trnková L (2004) Book of abstracts for XXIV International Scientific Opticalinary, Jetrichovice, Czech Republic. Czech Society, Praha, pp 69
21. Valléz E, Pollina R, Goméz J (1993) J Appl Electrochem 23:508
22. Goméz E, Muller C, Pollina R, Sarret M, Valléz E (1992) J Electroanal Chem 333:47
23. Turoňová T, Gálová M, Lux L, Gál M (2001) J Solid State Electr 5:502
24. Karwas C, Hepel T (1988) J Electrochem Soc 135:839
25. Karwas C, Hepel T (1989) J Electrochem Soc 136:1672